

Enhanced circular dichroism of TDBC in a metallic hole array structure

Tiantian He(何田田), Qihui Ye(叶起惠), Gang Song(宋钢)

Citation: Chin. Phys. B . 2020, 29(9): 097306 . **doi:** 10.1088/1674-1056/aba9ce
Journal homepage: http://cpb.iphy.ac.cn; http://iopscience.iop.org/cpb

What follows is a list of articles you may be interested in

Quantization of electromagnetic modes and angular momentum on plasmonic nanowires

Guodong Zhu(朱国栋), Yangzhe Guo(郭杨喆), Bin Dong(董斌), Yurui Fang(方蔚瑞)

Chin. Phys. B . 2020, 29(8): 087301 . **doi:** 10.1088/1674-1056/ab9698

Multiple Fano resonances in metal-insulator-metal waveguide with umbrella resonator coupled with metal baffle for refractive index sensing

Yun-Ping Qi(祁云平), Li-Yuan Wang(王力源), Yu Zhang(张宇), Ting Zhang(张婷), Bao-He Zhang(张宝和), Xiang-Yu Deng(邓翔宇), Xiang-Xian Wang(王向贤)

Chin. Phys. B . 2020, 29(6): 067303 . **doi:** 10.1088/1674-1056/ab888c

Optical spin-to-orbital angular momentum conversion instructured optical fields

Yang Zhao(赵阳), Cheng-Xi Yang(阳成熙), Jia-Xi Zhu(朱家玺), Feng Lin(林峰), Zhe-Yu Fang(方哲宇), Xing Zhu(朱星)

Chin. Phys. B . 2020, 29(6): 067301 . **doi:** 10.1088/1674-1056/ab862a

Selective excitation of multipolar surface plasmon in a graphene-coated dielectric particle by Laguerre Gaussian beam

Yang Yang(杨阳), Guanghua Zhang(张光华), Xiaoyu Dai(戴小玉)

Chin. Phys. B . 2020, 29(5): 057302 . **doi:** 10.1088/1674-1056/ab7e97

Research progress of femtosecond surface plasmon polariton

Yulong Wang(王玉龙), Bo Zhao(赵波), Changjun Min(闵长俊), Yuquan Zhang(张聿全), Jianjun Yang(杨建军), Chunlei Guo(郭春雷), Xiaocong Yuan(袁小聪)

Chin. Phys. B . 2020, 29(2): 027302 . **doi:** 10.1088/1674-1056/ab6717

Enhanced circular dichroism of TDBC in a metallic hole array structure*

Tiantian He(何田田)[1], Qihui Ye(叶起惠)[2], and Gang Song(宋钢)[3,†]

[1] School of Electronic Engineering, Beijing University of Posts and Telecommunications, Beijing 100876, China
[2] International School, Beijing University of Posts and Telecommunications, Beijing 100876, China
[3] School of Science, Beijing University of Posts and Telecommunications, Beijing 100876, China

(Received 19 May 2020; revised manuscript received 13 July 2020; accepted manuscript online 28 July 2020)

We investigate the enhanced chirality of chiral molecular J-aggregates (TDBC) by the propagating surface plasmons (PSPs) in the metallic hole array structure filled with TDBC. The two ends of the hole in the metal film form a low quality factor Fabry–Perot (FP) cavity, and this cavity confines PSPs. The resonant wavelength of the metallic hole array is tuned by the lattice constant and the size of the hole. Both the resonant wavelength of Ag hole array and the volume ratio of TDBC in the hybridized structure influence on the enhancement of the circular dichroism (CD) spectrum. The curve of CD spectrum shows Fano-like line-shape, due to the interaction between the non-radiative field in the FP cavity and the radiative field in chiral TDBC. The maximum of the CD spectrum of the hybridized structure is 0.025 times as the one of the extinction spectrum in a certain structure, while the maximum of the CD spectrum of TDBC is 1/3000 times as the one of the extinction spectrum. The enhanced factor is about 75. The resonant wavelength of the metallic hole array can be tuned in a large wavelength regime, and the chirality of a series of molecular J-aggregates with different resonant wavelengths can be enhanced. Our structure provides a new method to amplify the chirality of molecular J-aggregates in experiments.

Keywords: propagating surface plasmons, chirality, circular dichroism

PACS: 73.20.Mf, 87.64.Nj **DOI:** 10.1088/1674-1056/aba9ce

1. Introduction

Chirality and circular dichroism (CD) are very interesting properties of biomolecules.[1,2] In optical spectroscopy, the CD signals are used to illustrate conformational changes of biomolecules. Nonzero CD effect in a molecule shows if a molecule has neither mirror-symmetry planes nor a center of symmetry. Modern nanotechnology has the ability to assemble hybrid superstructures composed of nano-structures and biomolecules, which gives a new property of the hybridized structure.[3–7] In the near field regime, localized surface plasmons (LSPs) provide a new way to enhance the electromagnetic (EM) fields and enlarge the light and matter interaction. LSPs are the collective electric fields driven by the response of incident light in noble metallic nanostructures.[8–13] LSPs confine EM fields in the near field, but also enhance the chirality of molecules.[2,14–19] CD spectra of the hybridized structures made up of metallic nanostructures and chiral molecules are much larger than the one without metallic nanostructures.

The propagating surface plasmons (PSPs) are the electric wave along the interface between a metal and a dielectric, which are widely used in the enhanced transmission, the sensor devices, optical devices, and so on.[20–30] PSPs also have the ability to amplify EM fields at the interface between the metal and the dielectric medium. When PSPs go through an open end hole array, EM fields can be confined in the slot or the holes in a certain condition, which is tuned by both the size of the hole and the lattice constant of the array. These periodic structures are also used to achieve optical devices based on metasurface.[31–34] By tuning the geometric phase and plasmon retardation phase, the chirality of the devices and the orbital angular momentum generation are connected together. The structures are chiral and the materials are achiral. If chiral molecular J-aggregates such as TDBC are filled in the periodic holes, the chirality may be amplified by PSPs in a certain condition.

In this paper, we investigate the enhanced chirality of chiral molecular J-aggregates (TDBC) in a silver hole array structure. Chiral TDBC are filled in the holes. A chiral beam is injected into our proposed structure. The extinction spectrum and CD spectrum are obtained by the finite difference time domain (FDTD) method. The indies of both left hand and right hand TDBCs are obtained from experiment data. Our researches show a potential way to amplify the chirality of chiral molecular J-aggregates.

2. Calculation models and results

Our proposed structure is a square hole array in a silver film. Figure 1 depicts one unit of our proposed structure. The chemical formula and the absorption spectrum of chiral TDBC is also shown in Fig. 1. Chiral TDBCs are filled in the hole

*Project supported by the Fundamental Research Funds for the Central Universities and the National Key R&D Program of China (Grant No. 2016YFA0301300).
†Corresponding author. E-mail: sg2010@bupt.edu.cn
© 2020 Chinese Physical Society and IOP Publishing Ltd

with the size of $w \times w \times d$. The lattice constant of the hole array is l. A chiral beam is injected from the bottom of the structure. The permittivity of Ag is obtained from Ref. [35]. The dielectric constant of TDBC is described as[19]

$$\varepsilon_{\text{TDBC}} = \varepsilon_\infty + \sum_i \frac{f_i \omega_i^2}{\omega_i^2 - \omega^2 - \mathrm{i}\gamma_i \omega}, \tag{1}$$

where, i means left (L) or right (R). $\varepsilon_\infty = n_{\text{bg}}^2$, and $n_{\text{bg}} = 1.33$ is the index of the background. ω_i is the resonant frequency of TDBC, and γ_i is the damping constant of TDBC. f_i is the oscillator strength, which is influenced by the molar concentration of TDBC. ω is the frequency of incident light. According to the experiment measurement of TDBC, we obtain $\omega_{\text{L}} = 3.228 \times 10^{15}$ (rad/s), $\omega_{\text{R}} = 3.203 \times 10^{15}$ (rad/s), $\gamma_{\text{L}} = \gamma_{\text{R}} = 8.195 \times 10^{13}$ (rad/s), and $f_{\text{L}} = f_{\text{R}} = 0.01$, respectively.[19] The absorption of TDBC is shown in the inserted figure. There is a single smooth resonant peak in the absorption spectrum. The FDTD method is employed to simulate the extinction spectra and CD spectra. The gird of the structure is 5 nm. The extinction spectrum comes from $E_{\text{xt}} = 1 - T$, where T is the transmission. The CD spectrum comes from $\text{CD} = E_{\text{xt}_\text{L}} - E_{\text{xt}_\text{R}}$.

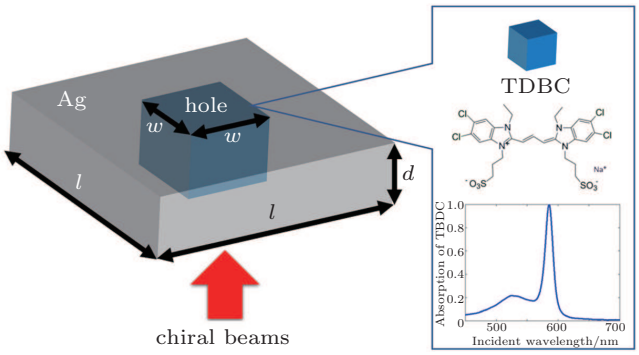


Fig. 1. The schematic diagram of the unit in our calculation structure.

In order to obtain the large interaction between the periodic Ag hole array structure and chiral TDBC, the resonant peaks of Ag hole array structure and TDBC should be close to each other. First, we choose the lattice constant l to be 560 nm and the width of the hole w is 400 nm. The thickness d of Ag film is 300 nm. The extinction spectrum E_{xt} and CD spectrum "CD" are shown in Fig. 2. We also simulate the structure with the air filled in the holes as shown in the inserted picture. As shown in Fig. 2(a), the asymmetric peak in the extinction spectrum due to the interaction between Ag hole array and chiral TDBC around the resonant wavelengths of chiral TDBC. As shown in the inserted picture, there is a symmetric peak at the wavelength of 582 nm, which is close to the resonant wavelengths of the chiral TDBC. The effective index at the ends of the hole structure is much larger than the one of the air. The holes in the film is treated as Febry–Perot (FP) cavities with a low quality factor involving the collective behavior.[20] The resonant wavelength of this FP cavity $\lambda_{\text{hole}}(d,l)$ is related with the thickness of the structure d and the lattice constant l. The optical characteristic of this structure β can be simply described as[36]

$$\beta = \frac{1}{\beta_{\text{hole}}(d) - S_k(l)}, \tag{2}$$

where β_{hole} describes the radiative and the dissipation of the fundamental mode as[37,38]

$$\beta_{\text{hole}} = \sqrt{1 - A\frac{1}{1 + F\sin(\phi)}}\, \mathrm{e}^{\mathrm{i}\phi}, \tag{3}$$

where A is the coefficients related to the length, the absorption of the hole, and the intensity reflectivity of the mirrors, F is the finesse, and ϕ is the phase shift of light passing through the hole, which is expressed as[37,38]

$$\phi = 2\pi \,\text{Re}(n_{\text{eff}})\frac{d}{\lambda}, \tag{4}$$

where, λ is the incident wavelength and it is the real part of the effective refractive index n_{eff} of the hole to PSPs.[39] $S_k(l)$ shows the collective behavior which is written as[36]

$$S_k = \sum \exp(\mathrm{i}k_0 l)\left[\frac{(1 - \mathrm{i}k_0 l)(3\cos^2\theta - 1)}{r^3} + \frac{k_0^2 \sin^2\theta}{r}\right], \tag{5}$$

where k_0 is the wave-vector in the vacuum, and θ is the in-plane angle between the hole locations. When the incident wavelength λ is equal to the lattice constant l, there is a dip in the extinction spectrum called Wood anomaly.[36,40] The parameter $\lambda_{\text{hole}}(d,l)$ is close to the value $\lambda = l$. Hence, we take the lattice constant l as 560 nm and the thickness d as 300 nm, and we may obtain that the resonant wavelength of Ag hole array is close to that of the chiral TDBC. In the extinction spectrum, there are several resonant peaks as shown in Fig. 2(a). The real part of the chiral TDBC index is quite larger or quite small than that of the air according to Eq. (1). Optical paths in the holes change a lot, and have the ability to form more resonant peaks. Also based on Eq. (4), the effective index of the square hole is influenced by the index of the medium in the hole. When the chiral TDBC is instead of the air, n_{eff} changes greatly around the resonant wavelength of the chiral TDBC and the fluctuated curves in Fig. 2 are mainly caused by the term of $\sin(\phi)$ in Eq. (3). The extinction spectrum reflects the resonance of the hybridized structure. In the Fabry–Perot cavity, all the resonant peaks of the extinction spectrum are related with the phase changes.[38] According to the analyses mentioned above, all resonant peaks in the extinction spectrum in Fig. 2(a) are related with ϕ in Eq. (3).

This Fabry–Perot cavity with air filled in the holes supports an EM fields' confinement at the resonant wavelength, and provides a dark mode EM field. We plot EM field intensity distributions in Figs. 2(c) and 2(d) to show the confinement of the hole array. The incident wavelengths are 560 nm ($T = 0.4$) and 582 nm (T close to 0), respectively. The EM field intensity is normalized to the incident intensity. Comparing the two

wavelengths, the EM field in the hole at $\lambda = 582$ nm is as about twice as the one at $\lambda = 560$ nm. The confinement of the EM field at $\lambda = 582$ nm is larger than the one at $\lambda = 560$ nm. The structure provides a non-radiative mode called the dark mode at the resonant wavelength.[41] These dark mode EM fields interact with bright mode EM fields offered by the chiral TDBC. Hence, the asymmetric peak is formed in the extinction spectrum of the hybridized structure.

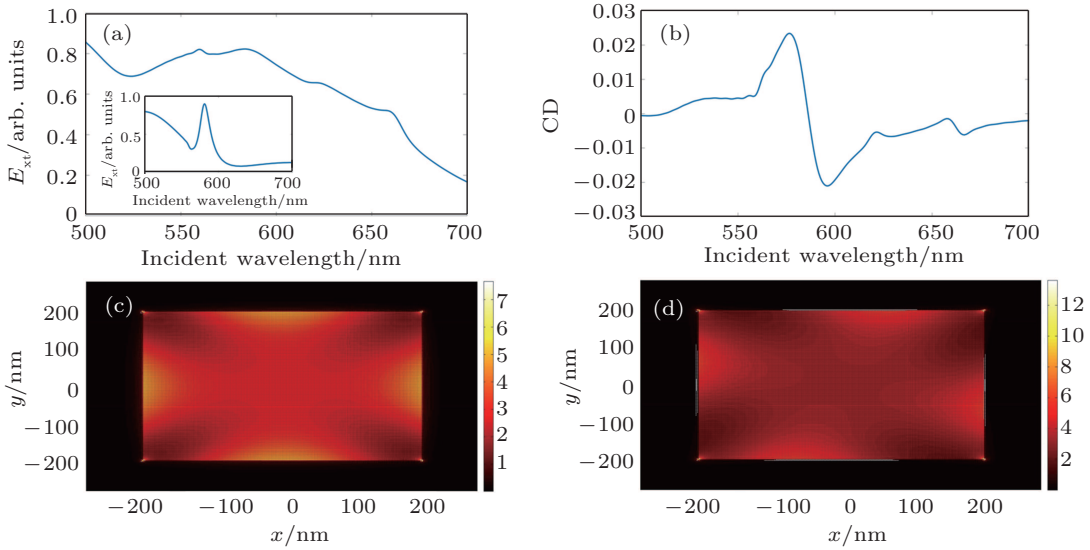


Fig. 2. The extinction spectrum (a) and CD spectrum (b) of our proposed structure with $l = 560$ nm and $w = 400$ nm, respectively. The EM field intensity distributions for Ag hole array structure with air at $\lambda = 560$ nm (c) and 582 nm (d), respectively. The insert plot is the extinction spectrum with the air filled in the hole.

The asymmetric peak is also observed in CD spectrum as shown in Fig. 2(b), which shows a Fano line shape curve. This also originates from the interaction between the dark mode EM fields provided by Ag hole array and the bright mode EM fields supported by chiral TDBC. The maximum of the absolute value in CD spectrum is as about 0.025 times as the maximum value in the extinction spectrum. The maximum value in only TDBC CD spectrum is as about 1/3000 times as the maximum of the extinction spectrum of TDBC. The CD spectrum is amplified by PSPs in our proposed structure. The incident light is squeezed at the interface between the hole array film and the air in form of PSPs. The PSPs amplify and confine EM fields at the resonant wavelength. The strong confined EM fields interact with TDBC. Hence not only the interaction between PSPs and TDBC is enhanced, but also the CD spectrum is enlarged. The previous works also report the enhancement of CD spectra and Fano curves in CD spectra in the hybridized structure composed of metallic nanoparticles and chiral molecules.[2,19] They use the large EM field amplification by LSPs. The ability of the EM field confinement for only PSPs is much weaker than the one for LSPs. Here, we use the metallic hole array to achieve FP cavities in order to realize the enhanced CD spectrum by PSPs. There are some previous works also focusing on the chirality based on PSPs.[31–34] They mainly create asymmetric structures to achieve the chirality. Comparing with these works, we concentrate on the chirality of the molecules in visible light and use achiral structure to amplify the chirality of the molecules.

Furthermore, in order to explore the interaction between the dark mode and the bright mode, we change the lattice constant l to show how the extinction spectrum and CD spectrum change. Here we choose $l = 520$ nm, 560 nm, 600 nm, and 640 nm, respectively. The extinction spectra and CD spectra are shown in Fig. 3. The other parameters are fixed.

As shown in Fig. 3(a), the extinction curve turns to be smooth around the resonant wavelengths of the chiral TDBC with the increase of the lattice constant l. The resonant wavelength of Ag hole array is tuned by the lattice constant. With the lattice constant increasing, the resonant wavelength has a red shift and is far away from that of the chiral TDBC, which changes from 553 nm ($l = 520$ nm) to 648 nm ($l = 640$ nm). The transmission value at $\lambda = 582$ nm rapidly decreases from 0.9 to 0.45 with the increase of l, and PSPs in the holes become weaker. The interaction between the dark mode EM fields and the bright mode EM fields is weakened around the resonant wavelengths of TDBC, and the line shape of the peak turns to be symmetric. The asymmetric peak is originated from the strong interaction between the structure and chiral TDBC in the condition of these two resonant wavelengths being close to each other. In Fig. 3(a), only the resonant wavelength of the structure with $l = 560$ nm is close to 582 nm. The resonant peak around 582 nm is asymmetric. The resonant peaks of other hybridized structures around 582 nm are symmetric. The asymmetric resonant peaks in Fig. 3(a) far away from the resonant peak of the chiral TDBC are mainly caused by the collective interaction among the FP cavities in the structure.

With the increase of l, Fano-like line shape in CD spectrum is also not obvious as shown in Fig. 3(b). The chirality

of TDBC has not been amplified due to weaker confinement of EM fields in the hole around the resonant wavelengths of TDBC. On the one hand, the Fano effect happens in the condition that the resonant wavelengths of both Ag hole array and chiral TDBC are close to each other. By increasing the lattice constant l, the resonant wavelength of Ag hole array is far away from that of the chiral TDBC, and the Fano effect gradually disappears. On the other hand, the volume ratio of TDBC in the hybridized structure also influences on CD spectrum. With the decrease of l, the volume ratio of TDBC increases, and the maximum value of CD spectrum shows a linear relationship with the volume ratio of TDBC.

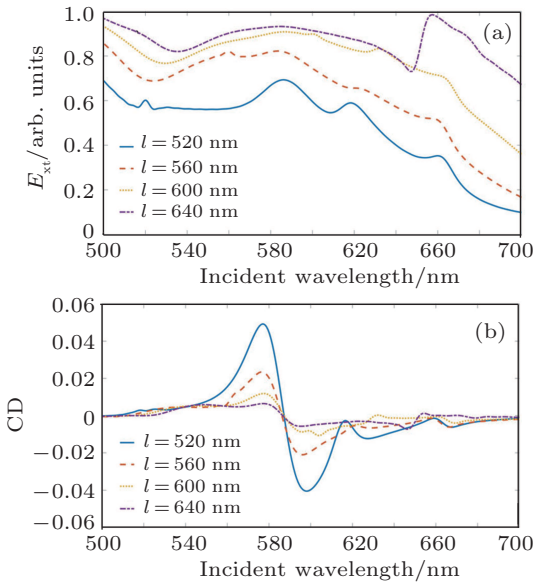


Fig. 3. The extinction spectra (a) and CD spectra (b) of our proposed structure with $w = 400$ nm and $l = 520$ nm, 560 nm, 600 nm, and 640 nm, respectively.

In order to illuminate our point of view as mentioned above, we fixed the lattice constant l at 560 nm, and tune the size w of the hole. The size w is adopted as 360 nm, 400 nm, 440 nm, and 480 nm, respectively. The results of extinction spectra and CD spectra are shown in Fig. 4.

As shown in Fig. 4(a), the resonant peak around $\lambda = 582$ nm is more obvious, and the intensity of the extinction decreases with the increase of w. The width of the hole w slightly modulates the resonant peak and has a great influence on the intensity of the extinction. With increasing w from 360 nm to 480 nm, the resonant wavelength changes from 575 nm to 600 nm and the extinction changes from 0.96 to 0.1 at $\lambda = 582$ nm. It means that there are more PSPs in the holes to interact with chiral TDBC. Hence, the CD spectrum increases linearly with w. The parameter w impacts on the quality factor of the FP cavity. With the size of w increasing, the real part of n_{eff} slightly increases by using mode analysis. Here, we can simply evaluate n_{eff} as $n_{\text{eff}} = [n_{\text{Ag}}(l^2 - w^2) + n_{\text{TDBC}}w^2]/l^2$, where n_{Ag} and n_{TDBC} are the indices of Ag and chiral TDBCs, respectively. Re$[n_{\text{Ag}}]$ is lower than 0.2 in visible light. With the increase of w, Re$[n_{\text{eff}}]$ is close to Re$[n_{\text{TDBC}}]$ and slightly increases. There is a little change in $\sin\phi$, and the optical path in Fabry–Perot gets longer. The resonant peak at $\lambda = 678$ nm in the structure with $w = 480$ nm supports our analyses above. The optical path becomes longer and the resonant peak appears in the long wavelength regime. In Fig. 4(a), with the width of the hole w increasing, the confinement of the hole turns to be weaker and the characteristic of the resonant peak for the hybridized structure is close to the resonant peak of the chiral TDBC around $\lambda = 582$ nm. Here, the resonant peak of the hybridized structure becomes symmetric around $\lambda = 582$ nm. The other asymmetric resonant peaks far away from the resonant peak of the chiral TDBC are mainly caused by the collective interaction among the FP cavities in the structure. Also, the interaction between the dark mode EM field and the bright mode EM field becomes weaker and the curves in both the extinction spectrum and CD spectrum become smooth. Due to the increase of the TDBC volume ratio, the maximum value of the CD spectrum linearly increases with parameter w.

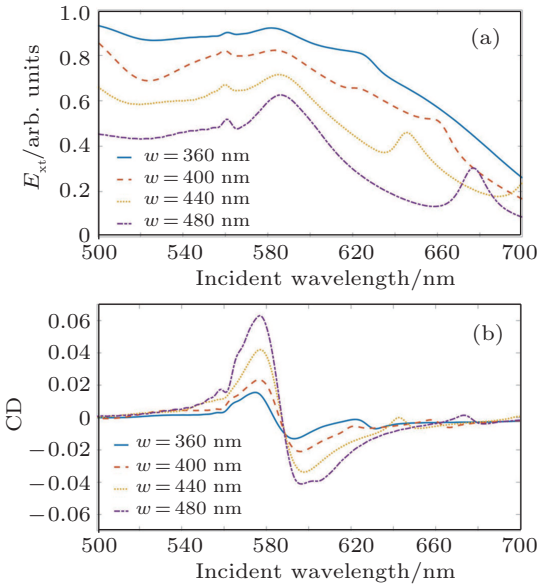


Fig. 4. The extinction spectra (a) and CD spectra (b) of our proposed structure with $l = 560$ nm and $w = 360$ nm, 400 nm, 440 nm, and 480 nm, respectively.

3. Summary

In summary, we reported on the enhanced chirality of TDBC by the PSPs in Ag hole array. The holes in Ag film form low quality factor of FP cavities and confines EM fields of the PSPs. The resonant wavelength of these FP cavities is tuned by the lattice constant and the size of the hole. Both the resonant wavelength of Ag hole array and the volume ratio of TDBC in the hybridized structure influence on the enhancement of the CD spectrum. The maximum value of the CD spectrum in the structure with $l = 560$ nm and $w = 400$ nm is as 75 times larger as that of only chiral TDBC. The resonant

wavelength of the metallic hole array can be tuned in a large wavelength regime, and the chirality of a series of molecular J-aggregates with different resonant wavelengths can be enhanced. Our proposed structure provides a new method to amplify the chirality of molecular J-aggregates in experiments.

References

[1] Webb R L 1996 *J. Med. Chem.* **39** 5285
[2] Govorov A O, Fan Z Y, Hernandez P, Slocik J M and Naik R R 2010 *Nano Lett.* **10** 1374
[3] Bruchez M P, Moronne M M, Gin P, Weiss S and Alivisatos A P 1998 *Science* **281** 2013
[4] Chan W C and Nie S 1998 *Science* **281** 2016
[5] Prodan E 2003 *Science* **302** 419
[6] Crookes-Goodson W J, Slocik J M and Naik R R 2008 *Chem. Soc. Rev.* **37** 2403
[7] Tang Y and Ouyang M 2007 *Nat. Mater.* **6** 754
[8] Scholl J A, Koh A L and Dionne J A 2012 *Nature* **483** 421
[9] Zhao Y, Xu L G, Ma W, Wang L B, Kuang H, Xu C L and Kotov N A 2014 *Nano Lett.* **14** 3908
[10] Qiang B, Dubrovkin A M, Krishnamoorthy H N S, Wang Q, Soci C, Zhang Y, Teng J H and Wang Q J 2019 *Adv. Photon.* **1** 026001
[11] Dai X Y, Yang Y and Zhang G H 2020 *Chin. Phys. B* **29** 057302
[12] Lu H, Xiao F J, Zhao J L, Zhang H M and Shang W Y 2018 *Chin. Phys. B* **27** 117301
[13] Jiang W, Xu Y H, Zhang S P, Xu H X, Chen W and Hu H T 2018 *Chin. Phys. B* **27** 107403
[14] Chervy T, Azzini S, Lorchat E, Wang S J, Gorodetski Y, Hutchison J A, Berciaud S, Ebbesen T W and Genet C 2018 *ACS Photon.* **5** 1281
[15] Alizadeh M H and Reinhard B M 2015 *ACS Photon.* **2** 1780
[16] Jiang Q B, Pham A, Berthel M, Huant S, Bellessa J, Genet C and Drezet A 2016 *ACS Photon.* **3** 1116
[17] Lan X and Wang Q B 2016 *Adv. Mater.* **28** 10499
[18] Caridad J M, Winters S, McCloskey D, Duesberg G S, Donegan J F and Krstić V 2018 *Nanotechnology* **29** 325204
[19] Song G, Guo J Q, Duan G Y, Jiao R Z and Yu L 2020 *Nanotechnology* **31** 345202
[20] Ruan Z C and Qiu M 2006 *Phys. Rev. Lett.* **96** 233901
[21] Song G, Li Y, Wu C,Duan G Y, Wang L L and Xiao J H 2013 *Plasmonics* **8** 943
[22] Song G, Yu L, Duan G Y and Wang L L 2017 *J. Phys. D: Appl. Phys.* **50** 205104
[23] Zou Y F, Song G, Jiao R Z, Duan G Y and Yu L 2019 *Nanoscale Res. Lett.* **14** 74
[24] Aneta P, Maciej C, Justyna G, Dorota K, Marcin N, Sebastian M and Dawid P 2018 *Nanoscale* **10** 12841
[25] Zhang D G, Xiang Y F, Chen J X, Cheng J J, Zhu L F, Wang R X, Zou G, Wang P, Ming H and Rosenfeld M 2018 *Nano Lett.* **18** 1152
[26] Kravets V G, Kabashin A V, Barnes W L and Grigorenko A N 2018 *Chem. Rev.* **118** 5912
[27] Wu Z H and Zhao T 2020 *Chin. Phys. B* **29** 034101
[28] Min C J, Zhang Y Q, Yang J J, Guo C L, Yuan X C, Wang Y L and Zhao B 2020 *Chin. Phys. B* **29** 027302
[29] Pang K W, Song G,Yu L and Li H H 2019 *Chin. Phys. B* **28** 127301
[30] Xiao Y C, Lu W, Yi H, Shi C, Jing X X, Li Z, Long H and Zeng X K 2019 *Chin. Phys. B* **28** 094215
[31] Guo Y H, Pu M B, Zhao Z Y, Wang Y Q, Jin J J, Gao P, Li X, Ma X L and Luo X G 2016 *ACS Photon.* **3** 2022
[32] Zhang F, Pu M B, Li X, Gao P, Ma X L, Luo J, Yu H L and Luo X G 2017 *Adv. Funct. Mater.* **27** 1704295
[33] Nemati A, Wang Q, Hong M H and Teng J H 2018 *Opto-Electron. Adv.* **01** 180009
[34] Mao L B,Liu K, Zhang S and Cao T 2020 *ACS Photon.* **7** 375
[35] Palik E D 1998 *Handbook of optical constants of solids*, Vol. 3 (Academic Press)
[36] Auguie B and Barnes W L 2008 *Phys. Rev. Lett.* **101** 143902
[37] Born M 1999 *Principles of optics — electromagnetic theory of propagation, interference and diffraction of light*, 7th edn. (DBLP)
[38] Shen Y and Wang G P 2008 *Opt. Express* **16** 8421
[39] Maier S A 2007 *Plasmonics: Fundamentals and Applications*, Vol. 2 (Spring Press)
[40] Wood R W 1902 *Proc. Phys. Soc. London* **18** 269
[41] Zhang S, Genov D A, Wang Y, Liu M and Zhang X 2008 *Phys. Rev. Lett.* **101** 047401